processes

MDPI

Article

Experimental Study on Methane Diffusion Characteristics of Different Metamorphic Deformed Coals Based on the Counter Diffusion Method

Jiangang Ren [1,2,*], Liang Gao [3], Zhihui Wen [4], Hongbo Weng [1], Jianbao Liu [1,2], Runsheng Lv [4], Yanwei Qu [1,4], Zhimin Song [1,2,4], Yongwang Zhang [1] and Bing Li [1,2,*]

[1] School of Environmental and Biological Engineering, Henan University of Engineering, Zhengzhou 451191, China; wengxiao211@163.com (H.W.); liujianbao342@126.com (J.L.); quyanwei@163.com (Y.Q.); songzhimin1961@hotmail.com (Z.S.); 17698828336@163.com (Y.Z.)
[2] Engineering Research Center of Resources and Ecological Environment Geology of Henan Province, Zhengzhou 451191, China
[3] No. 2 Geological Team, Hebei Coal Geology Bureau (Hebei Dry Hot Rock Research Center), Xingtai 054001, China; yuwengl@163.com
[4] State Key Laboratory Cultivation Base for Gas Geology and Gas Control, Henan Polytechnic University, Jiaozuo 454000, China; wenzhihui@hpu.edu.cn (Z.W.); lvrunsheng@hpu.edu.cn (R.L.)
* Correspondence: renjiangang2005@126.com (J.R.); hngclb@126.com (B.L.); Tel.: +86-137-2317-1269 (J.R.)

Abstract: The diffusion coefficient (*D*) is a key parameter that characterizes the gas transport occurring in coal seams. Typically, *D* is calculated using the desorption curve of particle coal. However, this method cannot accurately reflect the diffusion characteristics under the stress constraint conditions of in situ coal seams. In this study, different metamorphic deformed coals of medium and high coal rank were considered based on Fick's law of counter diffusion. The change laws of *D* under different confining pressures, gas pressures, and temperature conditions were tested and analyzed, and the influencing mechanisms on *D* are discussed. The results showed that *D* of different metamorphic deformed coals exponentially decreased with an increase in confining pressures, and exponentially increased with increases in gas pressures and temperature. There is a limit diffusion coefficient. The influence of the confining pressure on *D* can essentially be determined by changes in the effective stress, and *D* negatively affects the effective stress, similar to permeability. The effect of gas pressure on *D* involves two mechanisms: mechanical and adsorption effects, which are jointly restricted by the effective stress and the shrinkage and expansion deformation of coal particles. Temperature mainly affects *D* by changing the root-mean-square speed and average free path of the gas molecules. Under the same temperature and pressure conditions, *D* first increased and then decreased with an increase in the degree of deformation. *D* of the fragmented coal was the largest. Under similar deformation conditions, *D* of the high-rank anthracite was larger than that of the medium-rank fat coal. Porosity is a key factor affecting the change in *D* in different metamorphic deformed coals.

Keywords: counter diffusion method; confining pressure; gas pressure; temperature; diffusion coefficient

Citation: Ren, J.; Gao, L.; Wen, Z.; Weng, H.; Liu, J.; Lv, R.; Qu, Y.; Song, Z.; Zhang, Y.; Li, B. Experimental Study on Methane Diffusion Characteristics of Different Metamorphic Deformed Coals Based on the Counter Diffusion Method. *Processes* **2023**, *11*, 2808. https://doi.org/10.3390/pr11092808

Academic Editors: Chi-Min Shu, Junjian Zhang and Zhenzhi Wang

Received: 6 August 2023
Revised: 28 August 2023
Accepted: 19 September 2023
Published: 21 September 2023

1. Introduction

Increasing the efficiency of coalbed methane development and use can effectively alleviate the dependence on high-carbon energy, particularly coal, and accelerate the achievement of China's carbon peak and carbon neutrality goals. Within the context of the vigorous promotion of ecological environmental protection in China, the need to rapidly develop clean coalbed methane resources as substitutes for coal, which severely impacts on national safety and the natural environment, is becoming increasingly urgent [1,2]. China's coalbed methane resources rank third in the world at approximately 10.87×10^{12} m^3, demonstrating huge potential for coalbed methane resource development [3,4]. However, other

regions, except for the Qinshui Basin and the Ordos Basin, face low single-well yield, low production stability, and limited technical replicability during coalbed methane resource development. The core reasons for these issues are the features of the coalbed methane reservoirs in China, including low gas saturation, low permeability, low reservoir pressure, and the widespread development of tectonically deformed coal [5–7].

Coal is an extremely complex porous organic rock. According to the dual-porosity structure model of coal (Warren–Root model), the internal space of coal is composed of pores within and fractures around the coal matrix [8,9]. The pores and fractures in coal are storage spaces for coalbed methane and channels for methane migration [10,11]. Due to the differences in the causes, forms, and scales of pores and fractures in coal, the different migration mechanisms of methane in the pore and fracture channels can be divided into pore diffusion and fracture seepage [12,13]. Seepage can occur through the cleavage and fracture system in the coal body, which is driven by pressure differences, following Darcy's law [14,15]; diffusion can occur within the coal matrix pores and micro-fractures, which is driven by concentration differences, following Fick's law [16,17]. The coalbed methane production rate mainly depends on diffusion and seepage rates. When the diffusion rate is insufficient to provide the conditions necessary for seepage, the production rate is mainly controlled by the diffusion rate [18].

As the exploration and development of coalbed methane continue, the diffusion of methane in coal reservoirs has increasingly received attention. For coalbed diffusion media, two types of diffusion processes are observed in situ in coalbeds: columnar and particle coal sample diffusion [19,20]. Regarding the diffusion state, under certain temperature and pressure conditions, the three types of gas inside the coal matrix block that are not affected by mining are in a state of relative equilibrium. The force driving diffusion is the chemical gradient of self-diffusion [21]. If the reservoir pressure decreases, diffusion develops towards desorption, characterized by pressure relief gas extraction and coal drop gas gushing. If the reservoir pressure increases, diffusion develops toward adsorption, which is applied in N_2/CO_2 displacement technology. The force driving these two types of diffusion is the concentration gradient, which is a type of transfer diffusion [22,23]. Therefore, two types of diffusion media and three types of diffusion processes are observed in coalbeds under actual formation conditions, and different diffusion processes can coexist and transition into one another.

The diffusion coefficient (D) is a key parameter that controls the gas transport dynamics in the coal matrix. The existing methane diffusion coefficient measurement techniques include particle, steady-state flow, and counter diffusion methods, all of which have certain limitations and applications [4,18,24]. Different experimental methods of analyzing the process describe different diffusion processes. The particle method is a transient method used to measure the non-steady-state release of gas after the adsorption equilibrium pressure drops to atmospheric pressure. D is obtained via the inverse calculation of the coal gas desorption curve using a desorption model [24,25]. With this method, particle coal samples are used for testing, usually ignoring the influence of confining pressure. They are mainly used for gas content measurement (estimating the amount of gas lost during sampling) and predicting gas outbursts from coal drops [26,27]. The steady-state flow method used for obtaining D is similar to the steady-state flow method used for measuring the permeability of methane in coal. Cylindrical coal samples are used for the experiment; a constant methane pressure difference is maintained at both ends of the coal sample, and the methane diffusion coefficient in coal is calculated when the flow is stable according to the methane flow rate [18,28]. This method has not been widely used. Thimons and Sevenster measured the methane diffusion coefficient in coal using the steady-state flow method [29,30]. To address the problems of the long test times and the difficulty in avoiding methane seepage in coal with the steady-state flow method, Smith and Williams proposed measuring D of methane in coal using the constant-pressure counter diffusion method [31]. With the counter diffusion method, cylindrical coal samples are used for the experiment, placing methane and non-adsorptive nitrogen at both ends of the coal sample and ensuring

equal pressure. Because the gas pressure at both ends of the coal sample are equal, methane and nitrogen do not flow in the form of seepage; however, they diffuse with each other, driven by the concentration gradient. The methane concentrations at both ends of the coal sample are measured after a certain period to calculate the methane diffusion coefficient in the coal [32,33]. In counter diffusion experiments, confining pressure and gas pressure are simultaneously applied, using Fick's law to calculate D after data collection, and are mainly used to predict and evaluate the diffusion rate in the original coal seam, coalbed methane production planning, and economic reserve estimation. [34,35]. Scholars worldwide have conducted extensive exploratory studies of the measurement of gas diffusion coefficients. However, the experimental methods and results widely differ in the different studies when measuring D of methane in coal [26]. The methane diffusion coefficients in coal measured using different experimental methods considerably vary, with numerical ranges from 10^{-7} to 10^{-15} m^2/s. Differences in the testing principles and the conditions of different methods prevent the results of these techniques from being compared [36,37].

Due to the long geological history of coal seams, diffusion is an important mechanism for the underground migration and loss of gas in coal seams, and a method through which coalbed gas accumulates and is stored under the original stratum conditions. Many factors affect the gas diffusion in coal (coal particles), including the characteristics of the diffusion medium (coal characteristics, such as the state of matter, degree of metamorphism, degree of destruction, and microstructure), the diffusion phase (methane, such as gas concentration and molecular polarity of the gas), and the external environment (temperature, gas pressure, and confining pressure) [32,37–41]. Currently, most of the diffusion coefficients reported in the literature have been derived from adsorption data of particle coal based on Fick's classical homogeneous spherical mathematical diffusion model [4,37,40,42]. D or the adsorption time obtained using the particle method to evaluate gas diffusion in coal leads to substantial deviations from the actual gas diffusion characteristics and extraction rate [35,43]. In recent years, a few scholars have begun using columnar coal samples to measure diffusion coefficients. Meng & Li [32] used the counter diffusion method to determine the D values of low- to high-rank, original-structure coal, and they reported that from low- to medium-rank coal, the methane diffusion coefficient decreased as a negative exponential function with the increase in the degree of coal metamorphism. As the degree of coal metamorphism increased from medium- to high-rank coal, the methane diffusion coefficient exponentially increased. Under the same temperature, gas pressure, and confining pressure conditions, as the degree of coal metamorphism increased, the methane gas diffusion coefficient of the coal showed a trend of rapid decline, followed by a slow rise. Xu et al. [18] used thin slices of coal matrix instead of coal particles as their test samples and observed that the D value of the methane in the coal matrix first decreased and then increased with the increase in coal rank. Qin et al. [36] compared D measured using the steady-state method with the anthracite diffusion coefficient obtained using the classical model and the time-variable diffusion coefficient model; they observed that the magnitudes of the obtained diffusion coefficients were the same, the sizes differed by several-fold, and D showed different changes with the increase in methane pressure. Dong et al. [33] used the particle method and the counter diffusion method to measure the transient and quasi-steady-state diffusion characteristics of bituminous coal; their results showed that the quasi-steady-state diffusion coefficient was higher than the transient diffusion coefficient. This difference may have been related to the influence of adsorbed methane surface diffusion, suggesting that the transient diffusion coefficient should be used to calculate the coal and gas outburst risk evaluation index in gas extraction engineering. Liu et al. [35] studied the effects of confining pressure and pore pressure on the diffusion of methane in columnar coal samples. The results showed that the effective diffusion coefficient gradually decreased with an increase in the confining pressure and a decrease in the pore pressure. In future research, they suggested that block coal with a complete internal structure under constraints be used to study the methane diffusion behavior in situ coal seams. Cai et al. [44] observed the shape of coal fragments after crushing and sieving

a large number of coal samples, and found that most of the crushed particle coal was cylindrical- or rectangular-shaped, with a general particle size of 0.20–0.25 mm; a small amount of particle coal was spherical-shaped. Baatar et al. [34] determined the change in the coal body diffusion coefficient with confining and gas pressures using reverse diffusion experiments, and concluded that the internal pore/crack structure of the coal body strongly impacts on *D*.

Although *D* is a key parameter that characterizes the diffusion ability of methane in coal seams, the physical meaning, numerical magnitude, and changes in this parameter vary with laboratory test conditions. During gas extraction, methane diffuses into coal in two situations: (1) in coal particles, which is a transient diffusion process that occurs due to a high methane concentration gradient; and (2) in the coal matrix, where the methane concentration gradient is smaller, which can be regarded as a quasi-steady-state diffusion process. In situ coal seams are generally under stress constraints; however, researchers have often used granular coal to study the dynamic characteristics of methane diffusion, where the coal samples cannot withstand stress. Therefore, whether the laboratory test results of granular coal reflect the gas diffusion behavior of in situ coal seams is debatable. Moreover, reports are lacking on the determination of the methane diffusion coefficient using intact core samples of different metamorphic deformed coal in the laboratory using the counter diffusion method. To solve these problems, this study considered medium-to high-rank, original-structure coal and a series of tectonically deformed coal. Methane diffusion experiments were conducted on original coal columnar coal samples under different confining pressures, gas pressures, and temperature conditions using the counter diffusion method. The influence of confining pressure, gas pressure, and temperature on the methane diffusion characteristics of the original coal under stratum conditions was examined, and their relationship with porosity and the coal hardiness coefficient of outburst prevention was analyzed. The findings are scientifically valuable, enriching and improving the understanding of the gas migration of coal seam gas in coal seams in situ, CO_2-ECBM, and the geological sequestration of CO_2.

2. Experimental Design

2.1. Experimental Platform Construction

In the counter diffusion method, methane diffusion coefficient testers were used to simulate actual stratum conditions and determine the methane diffusion coefficient of an original coal seam under certain confining pressure, temperature, and gas injection pressure conditions. In this study, the *D* determination device consisted of a coal core holder, pressure control system, temperature control system, vacuum pump system, gas supply system, gas sampling device, and data collection system (Figure 1). The coal-core holder was used to fix the coal sample and provide a set-up for simulating the stratum pressure and temperature with the tested coal core. The pressure control system provided the circumferential and axial pressure required for the coal core in the experiment. The temperature control system provided constant temperature required for the coal core in the experiment. The gas supply system supplied CH_4 and N_2 to the gas chambers at both ends of the holder. The vacuum pump system provided a vacuum environment for the entire experimental system to ensure that the other gases in the system did not influence the results. After the experiment, a gas sampling device was used to collect gas samples for gas chromatography analysis. The data collection system was mainly used to collect experimental data such as the circumferential pressure, axial pressure, gas injection pressure, and temperature of the coal sample during the test. The experiment was based on the principle that gas freely diffuses through a coal sample under a concentration gradient. CH_4 was injected at one end and N_2 at the other end of the diffusion chamber of the coal sample holder; the pressure did not differ between ends. The gas concentration changed over time under the specified temperature and pressure conditions. Subsequently, the volume fraction values of each gas component in the diffusion chamber

at both ends at different time points were measured, and the methane diffusion coefficients of the different metamorphic deformed coals were calculated based on Fick's law.

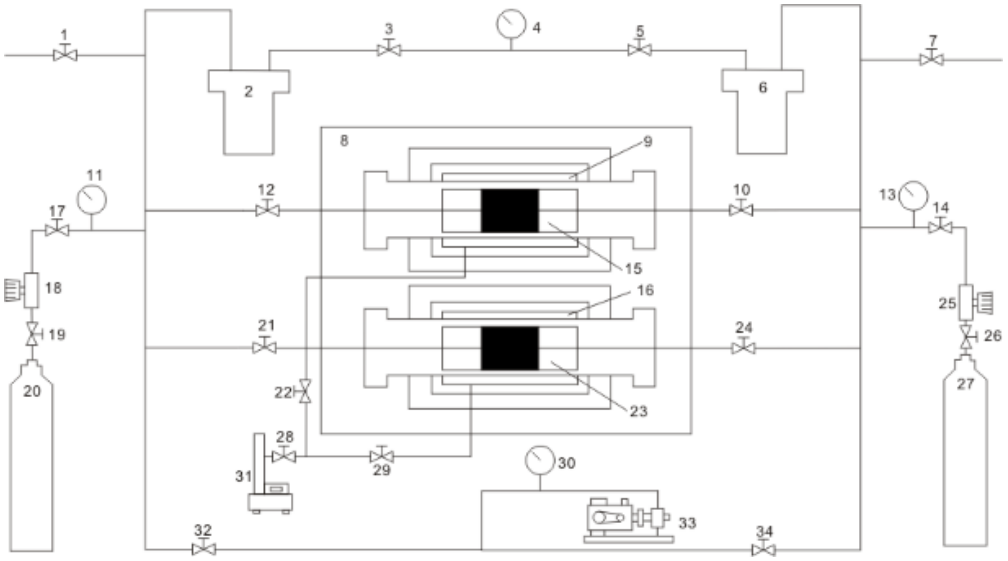

Figure 1. Diffusion coefficient determination device. Annotations: 1, 3, 5, 7, 10, 12, 14, 17, 19, 21, 22, 24, 26, 28, 29, 32, 34: shut-off valves; 2: methane chamber; 4: differential pressure transmitter; 6: nitrogen chamber; 8: coal core holder; 9, 16: confining pressure systems; 11, 13: pressure gauges; 15, 23: coal samples; 18, 25: pressure reducing valves; 20: CH_4; 27: N_2; 30: vacuum gauge; 31: confining pressure pump; 33: vacuum pump.

2.2. Experimental Samples

During their complex geological history and evolution, coal seams have undergone a series of metamorphic and deformation processes. Coal seams can thus be divided into original-structure coal and a series of tectonically deformed coal in terms of coal body structure types [3,45]. The experimental coal samples were collected from mining areas in the central and southern parts of north China, where the late Paleozoic Shanxi Group coal seams, original-structure coal, and tectonically deformed coal (fractured, granular coal, and mylonite coal) are well developed. Anthracite (No. WYM) from the Zhongmacun Mine in the Jiaozuo mining area, Henan Province, and fat coal (No. FM) from the No.12 mine in the Pingdingshan mining area, Henan Province, were collected. According to underground observations, the main coal seam in the Zhongmacun Mine, Coal 2-1, shows an interlayered distribution of four types of coal body structures, mainly developed in fractured coal and granular coal. The main coal seam in the No.12 mine, Coal 2-1, is mainly granular coal and mylonite coal, with local development of original-fractured structural coal. The coal body structure is original structural coal, fragmented coal, granulated coal, and mylonitic coal, numbered 1, 2, 3 and 4, respectively. The coal samples were labeled WYM-1, WYM-2, WYM-3, WYM-4, FM-1, FM-2, FM-3, and FM-4. According to Chinese national standards [46–49], 300 g of air-dried base coal samples with a size of 0.17–0.25 mm was selected from each sample, and the maximum vitrinite reflectance, industrial analysis, true density, apparent density, porosity, and coal hardiness coefficient parameters were determined. The results of the parameter determination are provided in Table 1.

Table 1. Basic parameters of coal samples.

Samples	Coal Structure	$R_{o,max}$ (%)	M_{ad} (%)	A_d (%)	V_{daf} (%)	FC_d (%)	Porosity/%	f Value
WYM-1	original-structure coal	3.38	2.94	8.41	5.50	83.15	6.25	1.19
WYM-2	fragmented coal	3.41	2.93	8.41	5.49	83.17	8.13	0.85
WYM-3	granulated coal	3.39	2.67	8.36	5.63	83.22	5.19	0.41
WYM-4	mylonitic coal	3.44	2.53	8.57	5.71	83.19	4.61	0.15
FM-1	original-structure coal	1.14	1.42	10.10	11.03	70.65	4.40	0.81
FM-2	fragmented coal	1.16	1.44	8.70	10.52	69.99	4.77	0.64
FM-3	granulated coal	1.14	1.21	8.65	10.79	70.52	3.32	0.31
FM-4	mylonitic coal	1.15	1.06	8.77	10.21	70.32	2.87	0.15

Note: M_{ad} is the moisture content, %; A_d, ash content, %; V_{daf} volatile content, %; FC_d fixed carbon content, %; f, solidity coefficient of coal (dimensionless).

Original cylindrical coal samples were used as the coal samples in this study. Four different types of coal body structures were prepared according to their hardness. For the harder original-structure coal and the fractured coal, core samples of the original cylindrical coal were directly prepared using a rock-core drill. For severely deformed structural coal (granulated and mylonite coal), which has a severely damaged structure, the cold isostatic pressing technique was used for coal sample preparation, simulating the overburden pressure when performing isostatic pressing molding. When forming the isostatic pressing test pieces, the isostatic pressure of the hydraulic system of the isostatic press was set according to Table 2 to simulate the overburden pressure needed to produce the original cylindrical samples of severely deformed structural coal. This method of creating original coal isostatic pressing test pieces of strongly deformed structural coal has several major advantages over conventional coal molding consolidation techniques (such as molding and extrusion), including simulating stratum pressure pressing, maintaining the original coal properties, enabling high-quality molding, providing easy sampling, and using simple processes. The method and steps for preparing the original isostatically pressed cylindrical coal samples with a strongly tectonic deformed were previously described [50]. The coal sample specifications were Φ25 mm × 50 mm. During the sample preparation process, the adverse effects of the different internal structures of the sample and the processing errors on the test results were avoided as much as possible. Additionally, the samples fabricated from the same piece of coal were selected using statistical classification and surface crack photography observation methods to select complete and compact samples and those without large exogenous cracks as experimental samples. After the samples were prepared, they were dried in an oven for 24 h. The original structural coal and the tectonically deformed coal columnar coal samples are shown in Figure 2.

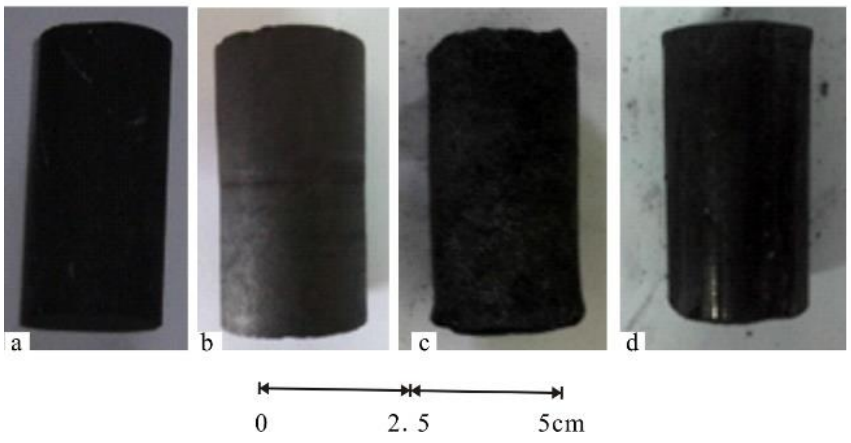

Figure 2. Original coal samples of four coal types used in the diffusion experiment: (**a**). original structural; (**b**). fragmented; (**c**). granulated; (**d**). mylonitic coal samples.

Table 2. Predicted results of the original coal seam temperature and pressure.

Coal Seam Burial Depth/m	Predicted Coal Seam Temperature/°C	Average Value/°C	Predicted Reservoir Pressure/MPa	Average Value/MPa
	Minimum/Maximum		Minimum/Maximum	
600	22/32	27	2.4/7.7	5.0
700	24/34	29	2.8/9.0	5.9
800	26/36	31	3.2/10.3	6.7
900	28/38	33	3.6/11.6	7.6
1000	30/40	35	4.0/12.9	8.6
1100	32/43	37.5	4.4/14.2	9.5
1200	34/46	40	4.8/15.5	10.3
1300	36/49	42.5	5.2/16.8	11.0

2.3. Experimental Conditions and Steps

(1) Prediction of coal seam temperature and pressure

Under the combined action of geothermal and overburden pressures, the temperature and pressure of the coal seam are linearly positively correlated with depth, and the geothermal and reservoir pressure gradient are the parameters reflecting this regular change. Reference [51] compiled the geothermal and reservoir pressure gradients of the main coal-bearing formations in China, including the Jiaozuo and Pingdingshan mining areas. The maximum, the minimum, and average geothermal gradients are 4.49, 0.40, and 2.12 °C/100 m, respectively. The maximum, the minimum, and average reservoir pressure gradients are 1.293, 0.402, and 0.862 MPa/100 m, respectively. The geothermal and reservoir pressure gradients of the Zhongmacun Mine and No.12 Pingdingshan Coal Mine do not demonstrate any geothermal or geopressure anomalies. They are basically at the average level in north China. Therefore, the temperature and pressure conditions of the coal seam at depths of 600–1300 m were predicted based on the average geothermal gradient and average reservoir pressure gradient of the coal-bearing strata in north China (Table 2).

Experiments were conducted based on the actual geological conditions, such as temperature, reservoir pressure, and gas pressure, during the exploration of in situ coal seams, combined with the purpose of this study and the pressure resistance of the coal samples. To determine the effect of individual variables (such as confining pressure, gas pressure, and temperature) on the CH_4 diffusion law of columnar coal samples, an orthogonal experimental design was applied according to Table 3. A comprehensive analysis followed this.

Table 3. Conditions for measuring *D* using the interdiffusion method.

Simulated Burial Depth/m	Confining Pressure/MPa	Gas Pressure/MPa	Temperature/°C	Remarks
600	5.0	0.5	27	Orthogonal experiment designed accordingly
800	6.7	1.0	31	
1000	8.6	1.5	35	
1200	10.3	2.0	40	

(2) Experimental procedure

The columnar coal sample to be tested was placed in a rock-core holder at a constant temperature, the gas chambers at both ends and the corresponding pipelines were installed and fixed, and a given environmental pressure was applied. The two gas chambers were subjected to a vacuum using a vacuum pump. After completing vacuuming, high-purity CH_4 and N_2 at equal pressures were simultaneously injected into the gas chambers on either side of the coal core. The pressures of the gases in the two gas chambers were adjusted to the designed pressure, the high-pressure valves on the gas chambers were closed, and gas diffusion began. After a certain period, samples were removed from the gases in the two gas chambers using the exhaust gas sampling method and analyzed using gas chromatography.

If the gas to be tested had diffused, the gas chamber was emptied, the experimental conditions were changed, and D was measured under new conditions; otherwise, the gas diffusion experiment was continued.

2.4. Calculation Models

The key parameter for measuring the diffusion capacity and speed of methane in coal is the diffusion coefficient $D(\mathrm{cm}^2/\mathrm{s})$. Quasi-steady-state diffusion occurs when the diffusion speed per unit area per unit time is proportional to the volume fraction gradient. The diffusion speed depends only on distance, irrespective of time, which follows Fick's first law. If the diffusion flux of methane in a coal seam varies with both time and distance, the diffusion is called non-steady-state diffusion, which can be described by Fick's second law. Therefore, D of methane in the experiment was calculated using Fick's second law (Equation (1)):

$$D = \frac{\ln(\Delta C_0/\Delta C_i)}{B(t_i - t_0)} \quad (1)$$

where: $\Delta C_i = C_{1i} - C_{2i}$, $B = A(1/V_1 + 1/V_2)/L$; D is the diffusion coefficient of the methane in the coal sample, cm^2/s; ΔC_0 is the volume fraction difference of the methane gas in the diffusion chamber at both ends at the initial moment, %; ΔC_i is the volume fraction difference of the methane gas in the diffusion chamber at both ends at the ith moment, %; t_i is the ith moment, s; t_0 is the initial moment, s; C_{1i} is the volume fraction of the methane gas in the methane diffusion chamber at the ith moment, %; C_{2i} is the volume fraction of the methane gas in the nitrogen diffusion chamber at the i^{th} moment, %; A is the cross-sectional area of the coal sample, cm^2; L is the length of the coal sample, cm; V_1, and V_2 are the volumes of the methane diffusion chamber and the nitrogen diffusion chamber, respectively, cm^3.

3. Results and Discussion

3.1. Influence of Confining Pressure on Diffusion Coefficient

A coal reservoir is a three-dimensional geological body stored underground at a certain depth, and its physical characteristics, especially diffusion and permeability, are closely related to the confining pressure [32,35]. Under natural conditions, the geostress field acts on the coal seam pores, forming a confining pressure on the coal seam pores, which affects the pore-fracture system of the coal seam and thus impacts the fluid migration laws in the coal seam. To measure the changes in D with changes in the confining pressure, samples WYM-1, WYM-2, WYM-3, WYM-4, FM-1, FM-2, and six original columnar coal samples were used in the experiments. The experiments were conducted under a confining pressure of 5.0, 6.7, 8.6, or 10.3 MPa; the temperature was 31 °C; and the gas pressure was 1.0 MPa. The experimental conditions and results are listed in Table 4.

Table 4. Impacts of confining pressure on D: experimental conditions and results.

Samples	Experimental Conditions			Effective Stress/MPa	CH_4 $D/(\mathrm{cm}^2/\mathrm{s})$	Samples	Experimental Conditions			Effective Stress/MPa	CH_4 $D/(\mathrm{cm}^2/\mathrm{s})$
	Confining Pressure/MPa	Temperature /°C	Gas Pressure/MPa				Confining Pressure/MPa	Temperature /°C	Gas Pressure/MPa		
WYM-1	5.0	31	1.0	4.0	7.44×10^{-8}	WYM-3	5.0	31	1.0	4.0	5.34×10^{-8}
	6.7			5.7	5.67×10^{-8}		6.7			5.7	4.12×10^{-8}
	8.6			7.6	3.86×10^{-8}		8.6			7.6	2.33×10^{-8}
	10.3			9.3	3.32×10^{-8}		10.3			9.3	1.84×10^{-8}
WYM-2	5.0	31	1.0	4.0	9.12×10^{-8}	WYM-4	5.0	31	1.0	4.0	4.53×10^{-8}
	6.7			5.7	6.85×10^{-8}		6.7			5.7	3.51×10^{-8}
	8.6			7.6	4.86×10^{-8}		8.6			7.6	2.23×10^{-8}
	10.3			9.3	4.32×10^{-8}		10.3			9.3	1.82×10^{-8}
FM-1	5.0	31	1.0	4.0	6.98×10^{-8}	FM-2	5.0	31	1.0	4.0	7.12×10^{-8}
	6.7			5.7	5.57×10^{-8}		6.7			5.7	5.65×10^{-8}
	8.6			7.6	3.75×10^{-8}		8.6			7.6	3.82×10^{-8}
	10.3			9.3	3.01×10^{-8}		10.3			9.3	3.09×10^{-8}

The experimental results in Table 4 were used to plot the relationship between D and the confining pressure in Figure 3. As shown in Figure 3, under constant temperature and gas pressure, the methane diffusion coefficient exponentially decreases with an increase in the confining pressure, and the rate of decrease slightly slows as the confining pressure continues to rise. When undamaged experimental coal samples were used, the confining pressure in the experiment was conducted to a limit of 10.3 MPa without slowing the rate of decline. When the confining pressure increased, D stabilized and no longer decreased.

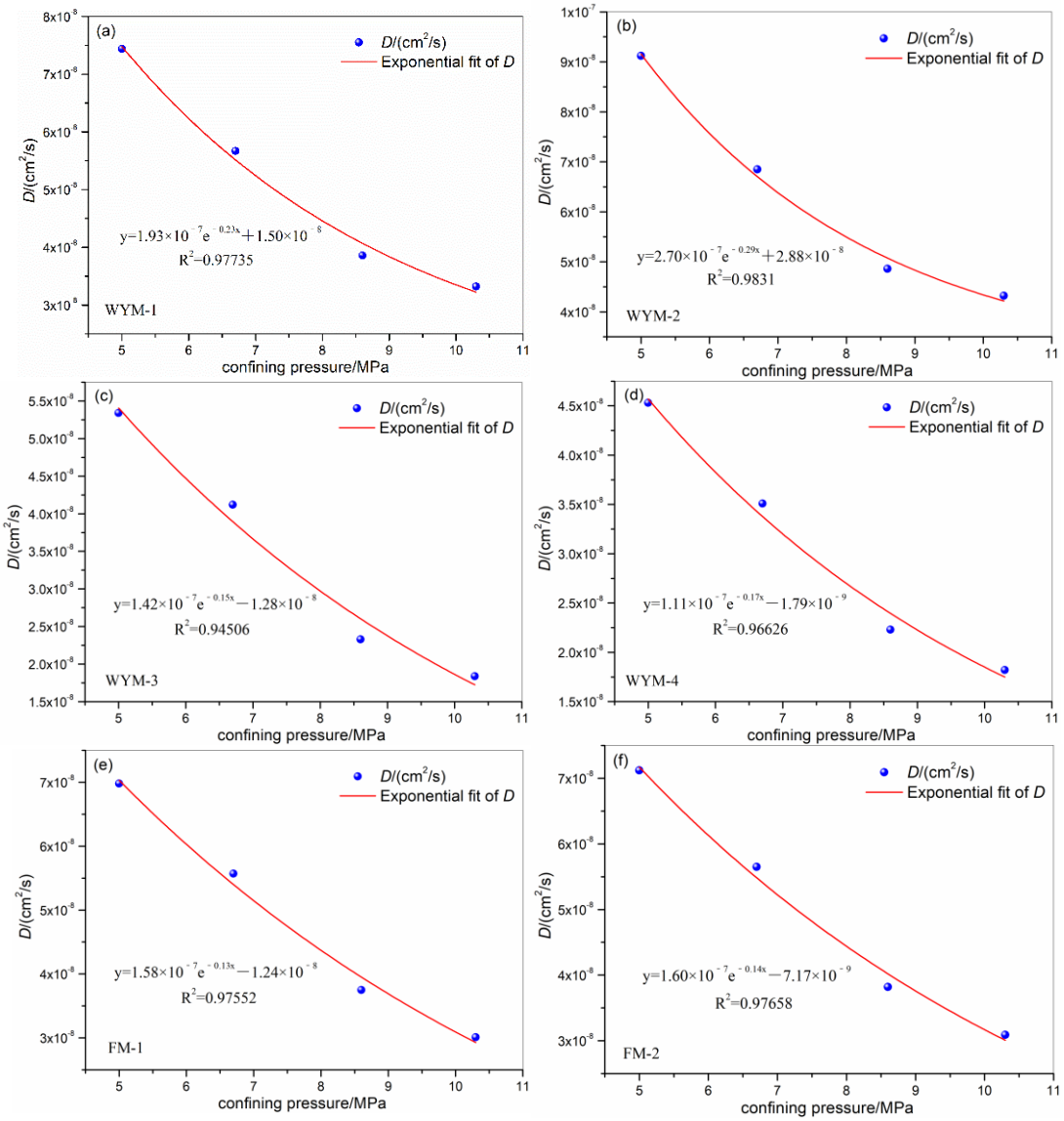

Figure 3. Relationship between D and confining pressure.

Effective stress refers to the difference between the confining pressure acting on a coal reservoir and the fluid pressure in its pores and fractures [26,35]. The data in Table 4 were used to plot the relationship between D and the effective stress generated by the change in the confining pressure (Figure 4). Figure 4 shows that the diffusion coefficient exponentially decreases with an increase in the effective stress, and the rate of decrease slightly slows as the effective stress increases. The exponential decrease in D with an increase in the confining pressure is thought to be determined by the change in the effective stress. According to the theory of material mechanics [52,53], coal deformation increases with stress. Therefore, when other conditions, including pore (gas) pressure, remain unchanged, as the confining pressure increases, the effective stress of the coal body continues to in-

crease, causing the coal body deformation to increase continuously. The pores and throats in coal contract and deform under the action of effective stress, ultimately leading to decreases in coal-body porosity and *D*. *D*, similar to permeability [12,54], negatively affects the effective stress.

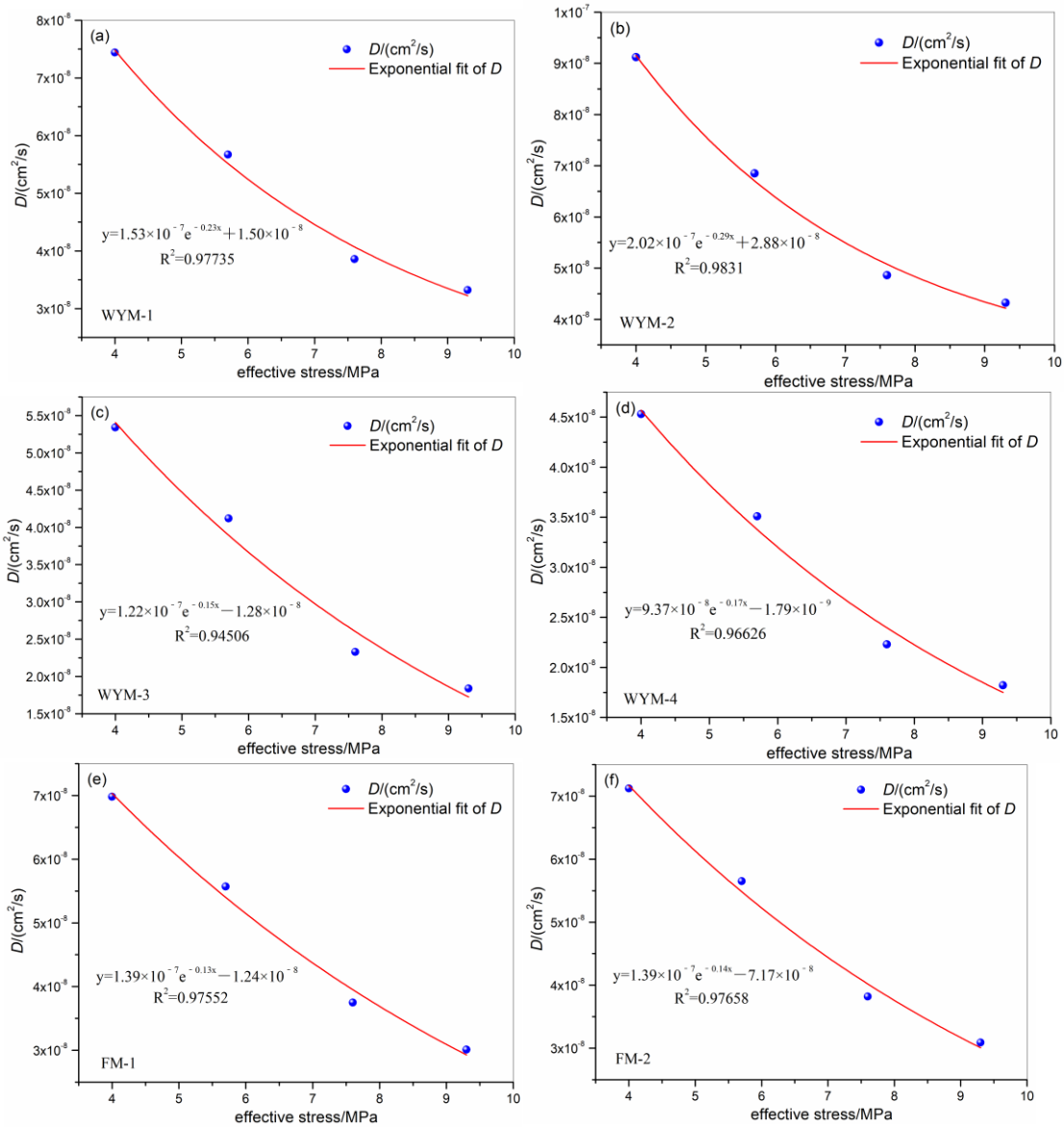

Figure 4. Relationship between *D* and effective stress (variable confining pressure).

3.2. Influence of Gas Pressure on Diffusion Coefficient

To explore the influence of changes in gas pressure on *D*, the change in *D* was measured using WYM-1, WYM-2, WYM-3, WYM-4, FM-1, FM-2, and six original columnar coal samples in the experiments. As shown in Table 3, the gas pressure was set to 0.5, 1.0, 1.5, or 2.0 MPa; the temperature was set to 31 °C; and the confining pressure was set to 6.7 MPa for the diffusion experiment. The experimental gas pressure conditions and results are summarized in Table 5.

Table 5. Effects of gas pressure on *D*: experimental conditions and results.

Samples	Experimental Conditions			Effective Stress/MPa	CH_4 D/(cm^2/s)	Samples	Experimental Conditions			Effective Stress/MPa	CH_4 D/(cm^2/s)
	Gas Pressure/MPa	Temperature/°C	Confining Pressure/MPa				Gas Pressure/MPa	Temperature/°C	Confining Pressure/MPa		
WYM-1	0.5	31	6.7	6.2	3.34×10^{-8}	WYM-3	0.5	31	6.7	6.2	3.01×10^{-8}
	1.0			5.7	5.67×10^{-8}		1.0			5.7	4.12×10^{-8}
	1.5			5.2	7.87×10^{-8}		1.5			5.2	6.12×10^{-8}
	2.0			4.7	8.46×10^{-8}		2.0			4.7	6.46×10^{-8}
WYM-2	0.5	31	6.7	6.2	4.23×10^{-8}	WYM-4	0.5	31	6.7	6.2	2.87×10^{-8}
	1.0			5.7	6.85×10^{-8}		1.0			5.7	3.51×10^{-8}
	1.5			5.2	8.12×10^{-8}		1.5			5.2	5.67×10^{-8}
	2.0			4.7	8.65×10^{-8}		2.0			4.7	5.98×10^{-8}
FM-1	0.5	31	6.7	6.2	3.14×10^{-8}	FM-2	0.5	31	6.7	6.2	3.35×10^{-8}
	1.0			5.7	5.57×10^{-8}		1.0			5.7	5.65×10^{-8}
	1.5			5.2	7.35×10^{-8}		1.5			5.2	7.67×10^{-8}
	2.0			4.7	7.67×10^{-8}		2.0			4.7	8.41×10^{-8}

The experimental results in Table 5 were used to plot the relationship between gas pressure and *D* (Figure 5). As shown in Figure 5, under constant temperature and confining pressure conditions, as the gas pressure increased from 0.5 to 2.0 MPa, the pattern of the change in the CH_4 diffusion coefficient of the six measured original columnar coal samples was opposite to that of the confining pressure, gradually increasing exponentially. The speed increase slowed as the gas pressure increased. When the gas pressure continued to increase, *D* tended to stabilize and no longer increase; therefore, a limited diffusion coefficient existed for the original columnar coal samples.

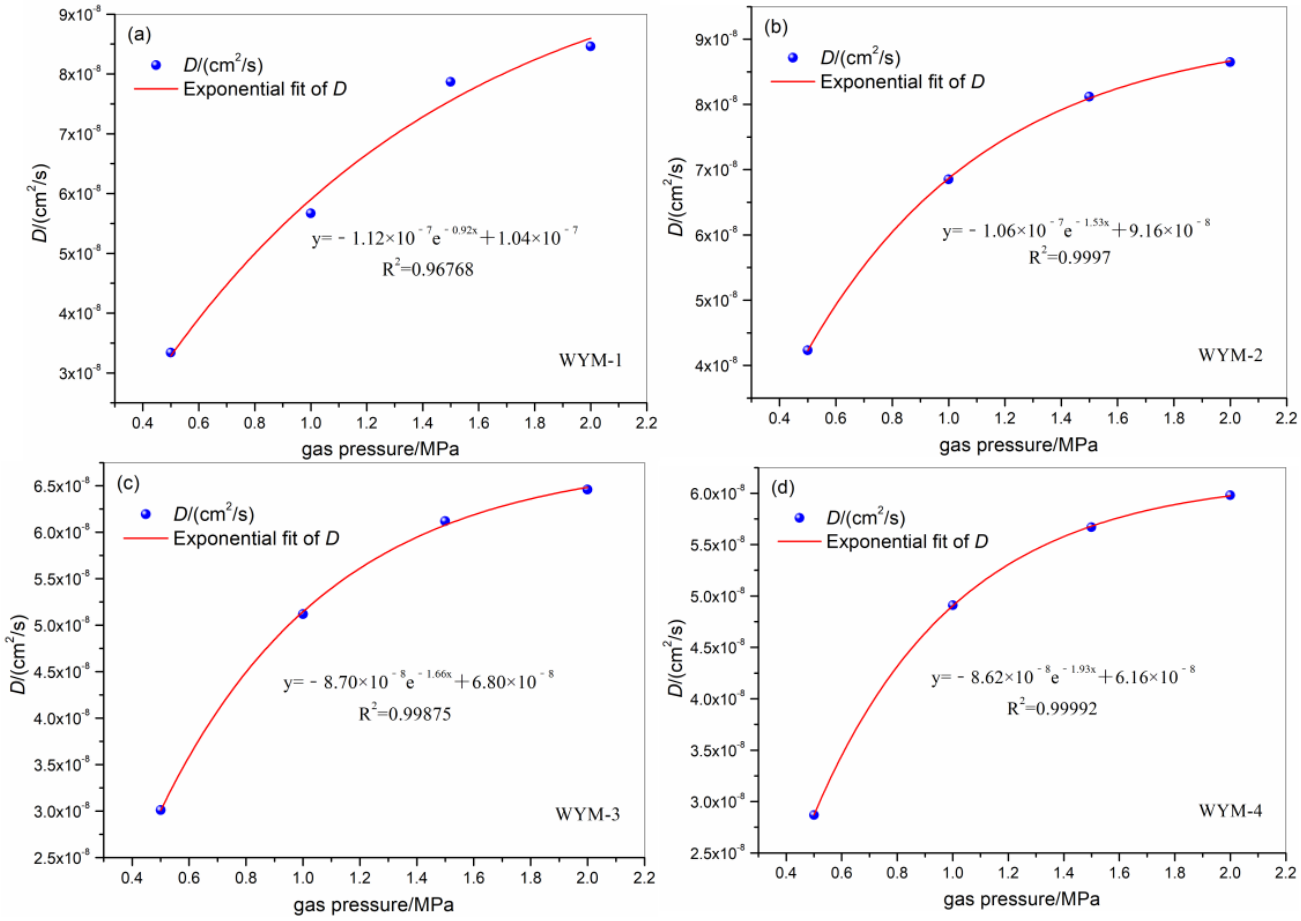

Figure 5. *Cont.*

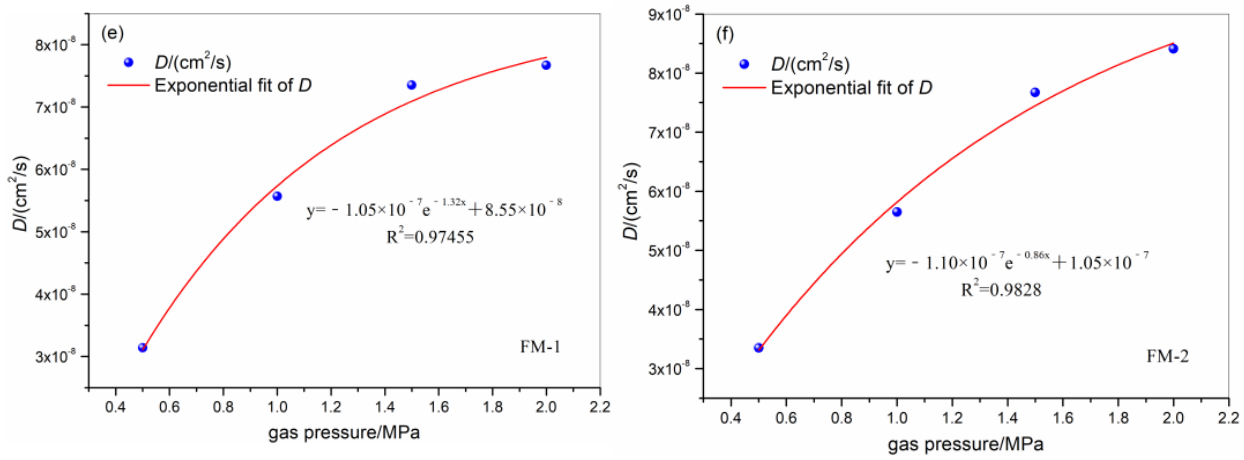

Figure 5. Relationship between *D* and gas pressure.

The experimental results in Table 5 were used to draw a graph of the relationship between *D* and the effective stress generated by the change in gas pressure (Figure 6). Figure 6 shows that the CH_4 diffusion coefficient of the original coal exponentially increases with a decrease in the effective stress, and the rate increase slightly slows as the effective stress decreases. The change in the effective stress determined the exponential increase in the CH_4 diffusion coefficient of the original columnar coal samples with increased gas pressure.

As the CH_4 gas pressure in coal increases, the coal adsorption of CH_4 gas molecules strengthens [55,56]. Under external constraint conditions, the adsorption expansion stress increases, leading to a decrease in the effective stress of the coal. As discussed in Section 3.1, decreased effective stress increases *D* (Figures 4 and 6). However, during the CH_4 diffusion process, the coal matrix exerts an adsorption effect on CH_4, with part of the adsorption expansion volume being converted into expansion stress at the contact points. Another part is converted into an inward adsorption expansion strain, which changes the pore volume. As the CH_4 gas pressure increases, the inward adsorption deformation of the coal matrix increases, the coal matrix expands, the porosity decreases, and *D* decreases. Conversely, when the pore pressure decreases, the coal matrix contracts, the porosity increases, and *D* increases. Therefore, compared with the influence of the confining pressure, the influence of the gas pressure on *D* involves two mechanisms: mechanical and adsorption actions.

The results of the experiments on the effects of changes in gas pressure on the original columnar coal samples showed that as the gas pressure increased, *D* increased. This indicates that the effective stress and the shrinking/expanding deformation of the coal matrix jointly constrain the effect of the gas pressure on CH_4 diffusion in coal. These two factors may yield opposite results; however, the dominant factor constrains the final relationship between the gas pressure and diffusion coefficient. The experiment results showed that the main factor influencing the change in the CH_4 diffusion coefficient in coal was the mechanical effect of effective stress.

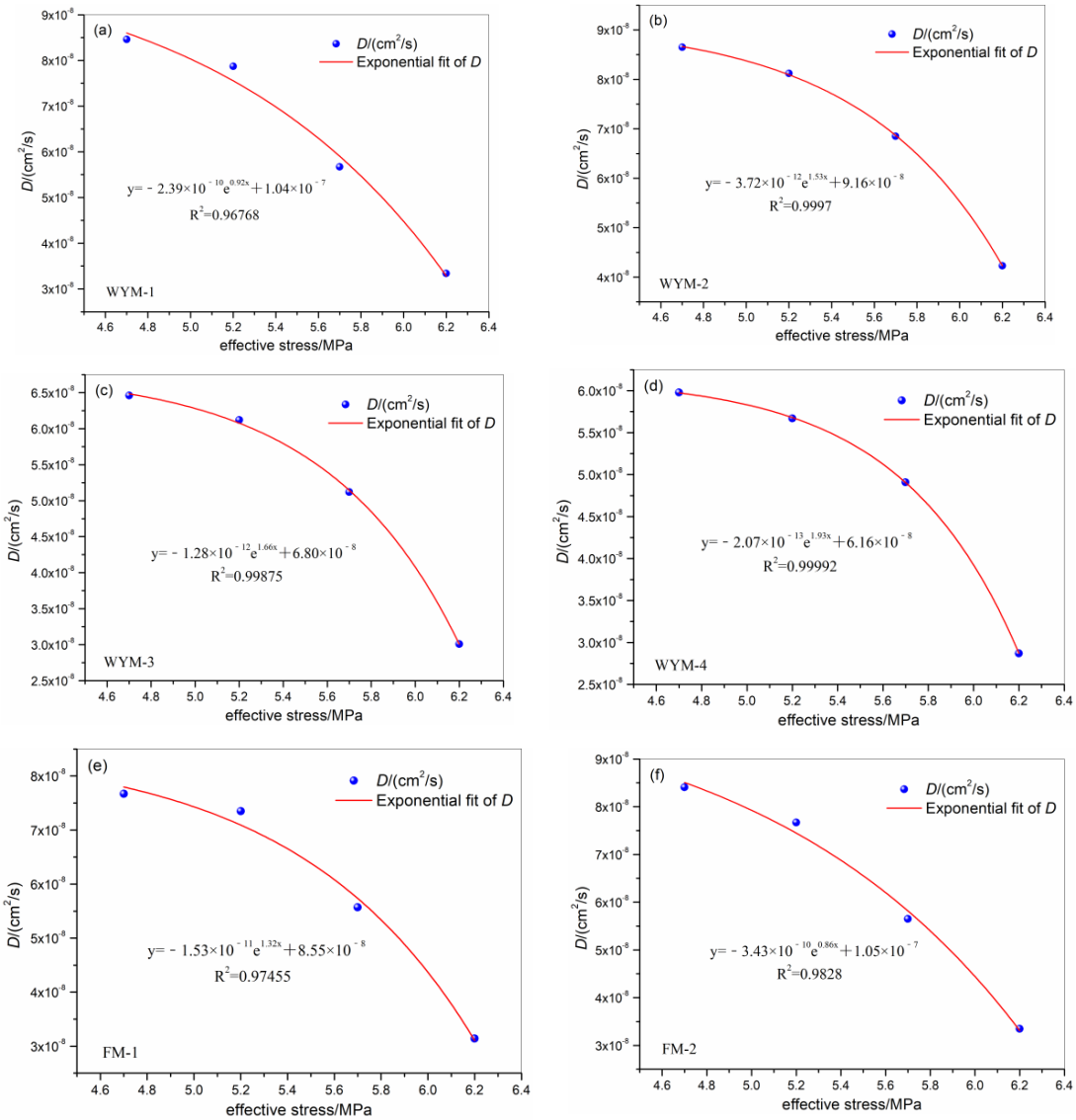

Figure 6. Relationship between *D* and effective stress (variable gas pressure).

3.3. Influence of Temperature on the Diffusion Coefficient

To explore the influence of changes in temperature on *D*, *D* was measured at various temperatures with the WYM-1, WYM-2, WYM-3, WYM-4, FM-1, FM-2, and six original coal columnar coal samples. For the experiment, the temperature was set to 27, 31, 35, 40, 45, or 50 °C; the confining pressure was 6.7 MPa; and the gas pressure was set to 1.0 MPa. The experimental conditions and results are listed in Table 6. The data in Table 6 were used to plot a graph depicting the relationship between *D* and temperature (Figure 7).

Table 6. Effects of temperature on *D*: experimental conditions and results.

Samples	Experimental Conditions			CH_4 $D/(cm^2/s)$	Samples	Experimental Conditions			CH_4 $D/(cm^2/s)$
	Temperature/°C	Confining Pressure/MPa	Gas Pressure/MPa			Temperature/°C	Confining Pressure/MPa	Gas Pressure/MPa	
WYM-1	27	6.7	1.0	5.62×10^{-8}	WYM-3	27	6.7	1.0	4.07×10^{-8}
	31			5.67×10^{-8}		31			4.12×10^{-8}
	35			5.73×10^{-8}		35			4.18×10^{-8}
	40			5.83×10^{-8}		40			4.27×10^{-8}
	45			5.97×10^{-8}		45			4.43×10^{-8}
	50			6.19×10^{-8}		50			4.56×10^{-8}

Table 6. *Cont.*

Samples	Experimental Conditions			CH_4 $D/(cm^2/s)$	Samples	Experimental Conditions			CH_4 $D/(cm^2/s)$
	Temperature/°C	Confining Pressure/MPa	Gas Pressure/MPa			Temperature/°C	Confining Pressure/MPa	Gas Pressure/MPa	
WYM-2	27	6.7	1.0	6.81×10^{-8}	WYM-4	27	6.7	1.0	3.46×10^{-8}
	31			6.85×10^{-8}		31			3.51×10^{-8}
	35			6.91×10^{-8}		35			3.55×10^{-8}
	40			7.03×10^{-8}		40			3.62×10^{-8}
	45			7.16×10^{-8}		45			3.70×10^{-8}
	50			7.34×10^{-8}		50			3.81×10^{-8}
FM-1	27	6.7	1.0	5.54×10^{-8}	FM-2	27	6.7	1.0	5.62×10^{-8}
	31			5.57×10^{-8}		31			5.65×10^{-8}
	35			5.63×10^{-8}		35			5.72×10^{-8}
	40			5.69×10^{-8}		40			5.78×10^{-8}
	45			5.76×10^{-8}		45			5.85×10^{-8}
	50			5.86×10^{-8}		50			5.96×10^{-8}

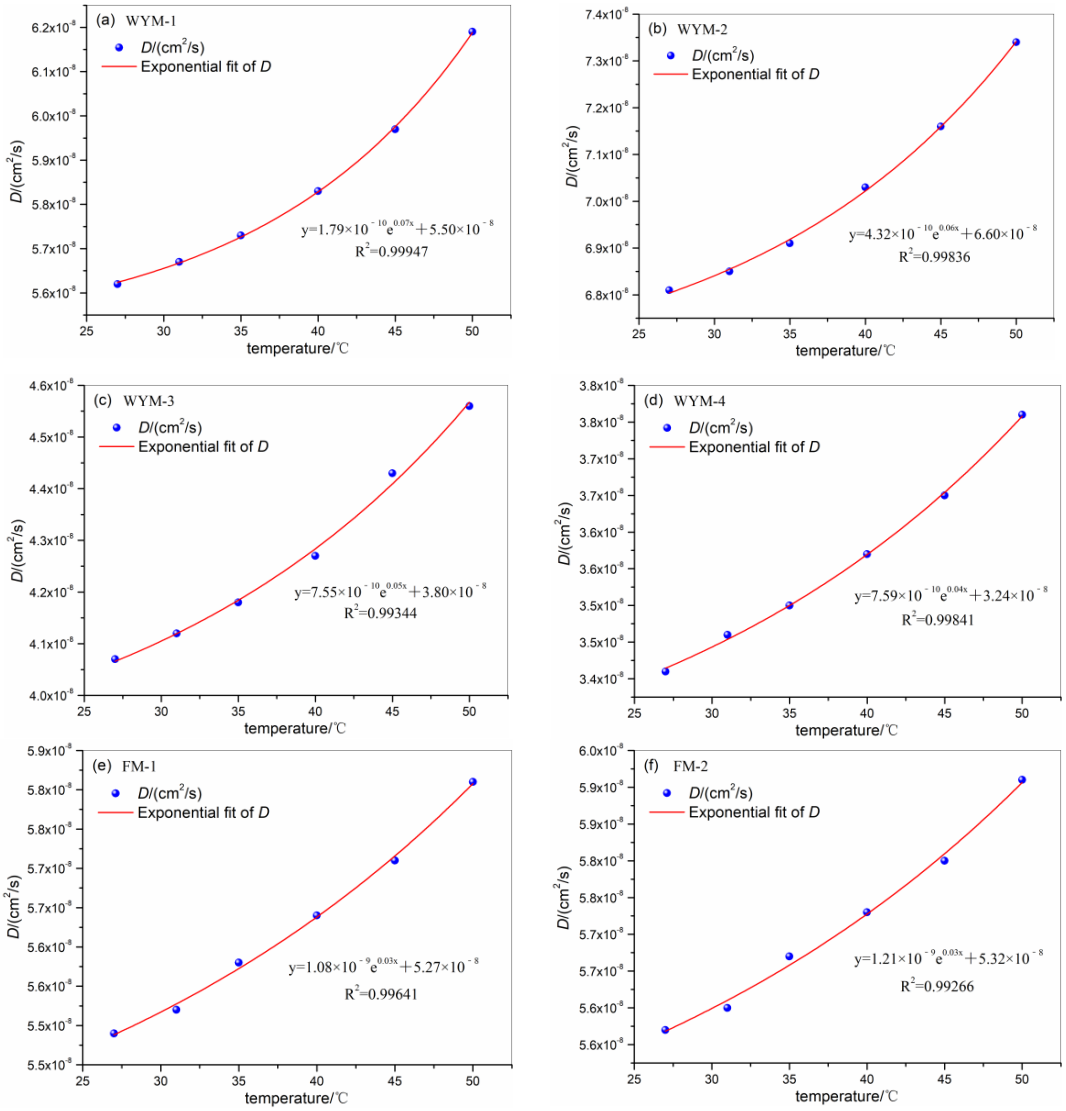

Figure 7. Relationship between *D* and temperature.

As shown in Figure 7, under constant gas and confining pressure conditions, as the temperature increased from 27 to 40 °C, the change in the pattern of the CH_4 diffusion coefficient in the six coal samples gradually and exponentially increased. Furthermore, as the temperature increased, the rate of increase slightly accelerated.

According to the theory of gas molecular motion [57,58], temperature mainly impacts gas molecular diffusion through the root-mean-square speed and average free path of the gas molecules. Molecular motion theory in materials science states that the temperature of a gas is an indicator of the average kinetic energy of the molecules [32,59]. As temperature increases, the amplitude and frequency of molecular vibrations, the speed of molecular motion, the vigor of molecular movement, and the speed of movement from high to low concentrations all increase. These, in turn, accelerate diffusion, ultimately causing *D* to trend upward.

3.4. Influence of Metamorphism and Deformation Degree on the Diffusion Coefficient

To determine the influence of the degree of metamorphism and deformation on *D*, the original columnar coal samples with different degrees of metamorphism and deformation were analyzed using WYM-1, WYM-2, WYM-3, WYM-4, FM-1, FM-2, FM-3, FM-4, and eight original coal samples. The confining pressure, temperature, and gas pressure were set to 6.7 MPa, 31 °C, and 1.0 MPa, respectively, to simulate a coal seam buried 800 m deep. Then, the confining pressure temperature and gas pressure were set to 8.6 MPa, 35 °C, and 1.5 MPa, respectively, to simulate a coal seam buried 1000 m deep. The experimental conditions and results are listed in Table 7.

Table 7. Effects of different metamorphic deformation degree on *D*: experimental conditions and results.

Samples	*f* Value	Experimental Conditions			CH_4 *D*/(cm^2/s)	Simulated Coal Seam Burial Depth/m
		Confining Pressure/MPa	Temperature/°C	Gas Pressure/MPa		
WYM-1	1.19	6.7	31	1.0	5.67×10^{-8}	800 m
WYM-2	0.85	6.7	31	1.0	6.85×10^{-8}	
WYM-3	0.41	6.7	31	1.0	4.12×10^{-8}	
WYM-4	0.15	6.7	31	1.0	3.51×10^{-8}	
FM-1	0.81	6.7	31	1.0	5.57×10^{-8}	
FM-2	0.64	6.7	31	1.0	5.65×10^{-8}	
FM-3	0.31	6.7	31	1.0	3.78×10^{-8}	
FM-4	0.15	6.7	31	1.0	3.24×10^{-8}	
WYM-1	1.19	8.6	35	1.5	4.38×10^{-8}	1000 m
WYM-2	0.85	8.6	35	1.5	5.46×10^{-8}	
WYM-3	0.41	8.6	35	1.5	2.83×10^{-8}	
WYM-4	0.15	8.6	35	1.5	2.53×10^{-8}	
FM-1	0.81	8.6	35	1.5	4.25×10^{-8}	
FM-2	0.64	8.6	35	1.5	4.73×10^{-8}	
FM-3	0.31	8.6	35	1.5	2.56×10^{-8}	
FM-4	0.15	8.6	35	1.5	2.14×10^{-8}	

The data in Table 7 were used to graph *D* for different degrees of metamorphism and deformation of the coal methane (Figure 8). As shown in Figure 8, under the same confining pressure, temperature, and gas pressure conditions, *D* of metamorphic coal (anthracite and fat coal) initially increased, which was followed by a decreasing trend with an increase in the degree of deformation, with the *D* value of fragmented coal being the largest. Coals with similar degrees of deformation had *D* that showed an increasing trend with increasing metamorphism degree; under the same degree of deformation, *D* of anthracite was larger than that of fat coal. *D* measured via the granular method [13,60] continuously increased with an increase in the degree of coal deformation, which differs from the finding obtained from counter diffusion experiments with different degrees of columnar coal sample metamorphism and deformation.

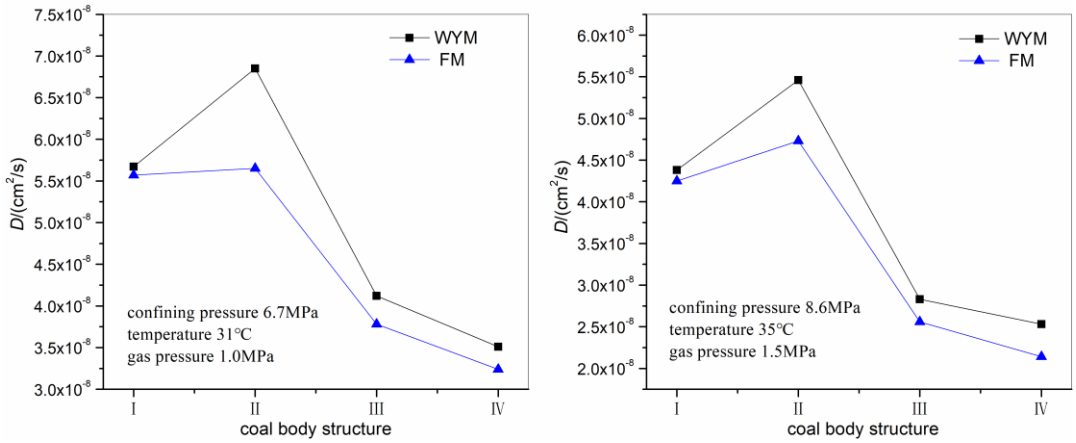

Figure 8. Change in D for different metamorphic deformation coal.

The solidity coefficient of coal (f) indicates its solidity. The drop hammer method is commonly used in China to determine f. The principle of this measurement method is based on brittle materials following area–force energy theory when they break. The work A consumed by broken coal is assumed to be directly proportional to the surface area S of the broken material, and the surface area is inversely proportional to the particle diameter. The crushing ratio can express coal solidity: the harder the coal, the higher its strength and the larger its f, and vice versa.

The f is an index that reflects the ability of coal to resist damage due to external forces. The f value of coal with different structural types ranges within certain values and a relatively dense interval, a common value range. Therefore, the f value can be used as an index for classifying coal structures. Using the data in Tables 1 and 7, the relationship between D of coal with different coal body structures and f was drawn, as shown in Figure 9.

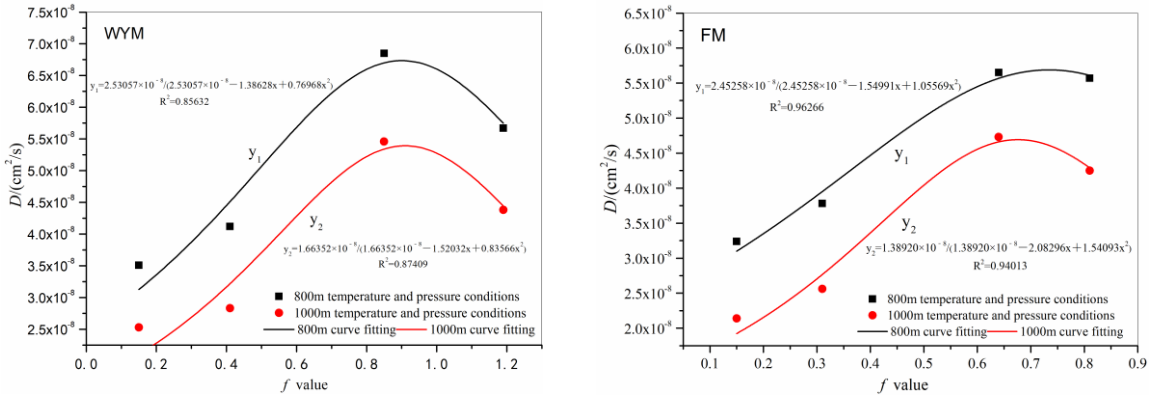

Figure 9. Relationship between D and f values of different metamorphic deformation coals.

Figure 9 shows that the following functional relationship can express the relationship between D and f:

$$D = a/(a + b \cdot f + c \cdot f^2) \quad (2)$$

where D is the diffusion coefficient, cm^2/s; f is the solidity coefficient of coal (dimensionless); and a, b, and c are dimensionless undetermined coefficients.

This shows that D and f are strongly correlated, with a determination coefficient (R^2) above 85%; therefore, the f value of coal can be used to predict D of coal. The structure of the coal changed from simple to complex, and D first increased and then decreased, indicating a nonlinear Holliday functional relationship.

The data in Tables 1 and 7 were used to plot the changes in the relationship between D of different metamorphic deformed coals and porosity under simulated confining

pressure, temperature, and gas pressure conditions at burial depths of 800 and 1000 m (Figure 10). As shown in Figure 10, *D* and the porosity of coal with different degrees of metamorphic deformation exhibited the same trend; that is, for the same coal ranking, with an increase in the degree of deformation, *D* and porosity both showed a trend of first increasing and then decreasing. For the same coal rank, the porosity and *D* of fragmented coal were the highest, followed by those of the original-structure coal and granular coal. *D* of granulated coal was the smallest. For the same degree of deformation, the porosity and *D* of anthracite were larger than those of fat coal.

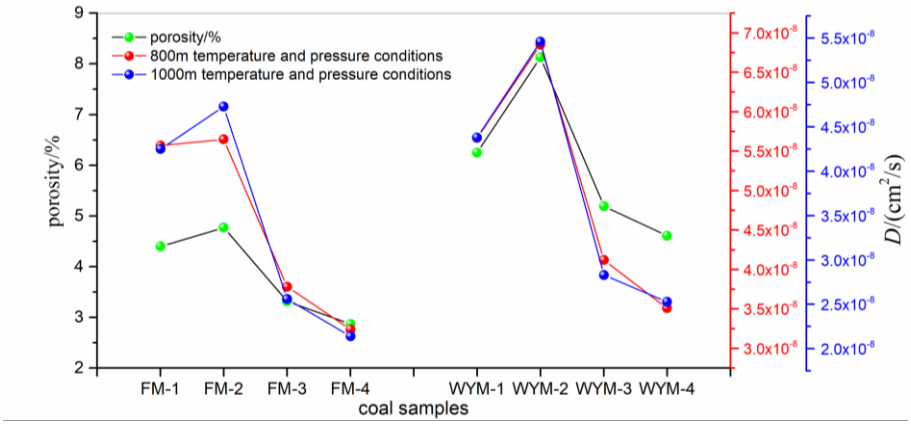

Figure 10. Relationship between *D* and porosity of different metamorphic deformation coals.

The effects of metamorphism and deformation are inseparable during the coal-forming process of a coal seam. Coal porosity refers to the ratio of the voids, including micropores and microfractures, in the coal to its total volume (GB/T23561.4-2009) [61]. The porosity measurements of the coal samples in Table 1 show that under the same metamorphic conditions, the porosity of different grades of coal was the highest in fragmented coal; with the increase in deformation degree, the porosity first increased and then decreased. This occurs because, in coal-bearing strata near the same location, the coalification history and process experienced by the coal seam were almost the same, the degree of coal metamorphism was essentially the same, and the confining pressure conditions were similar. Under the same stratum pressure conditions, a coal seam with a larger deformation degree (granular coal and mylonitic coal) is more likely to be compacted and solidified, resulting in smaller macroporosity. In contrast, a coal seam with a smaller degree of deformation (original structure or fragmented coal) has a stronger ability to maintain its original structure. As a result, it is less likely to be compacted; additionally, the original pores and microfractures are better preserved, and the porosity of fragmented coal is relatively high. The higher the porosity, the lower the displacement pressure, indicating the presence of more coarse throats and better pore structure, which are more conducive to diffusion. Conversely, the weaker the pore structure, the more unfavorable the diffusion [8,27,38]. *D* measured in the columnar coal samples in the counter diffusion experiment was mainly controlled by porosity, where large pores and microfractures were leading. Microfractures constitute important channels for connected pores, endogenous fractures, and layer fractures; the existence of microfractures shortens the distance required for coal seam methane diffusion [45,53,54]. In addition to the diffusion in micropores and flow in endogenous fractures, coal seam methane can diffuse or flow into microfractures. The analysis results indicated that whether seepage occurs in coal seams depends on the size of the diffusion channels in the coal seams and whether the coal seam provides the mechanical conditions for seepage to occur. In other words, even in large pores and microfractures, the mechanical condition may be unsuitable for seepage to occur in and out of the coal seam (i.e., the start-up pressure gradient) [4,62] or the microfractures to be partially filled. In this situation, the residual voids are insufficient for the methane to flow in the coal seam; as a result, this methane moves through the microfractures in the form of diffusion. Under these condi-

tions, the microfracture size is the key determinant of the diffusion of coal seam methane. Macromanifestation occurs when the permeability of soft coal under reservoir conditions is lower than that of hard coal. This explains why soft coal is more difficult to extract, why the effect of gas injection displacement is weak, and why the macrotransformation of hydraulic fracturing is difficult. Therefore, in future research, columnar coal samples with different degrees of metamorphic deformation under the action of effective stress should be used to study the diffusion behavior of in situ coal seam gas. The diffusion coefficients measured using the particle and counter diffusion methods cannot be simply substituted in practical situations.

4. Conclusions

(1) The methane D of the raw coal cylindrical samples exponentially decreased with increasing confining pressure, and the decrease slightly slowed as the confining pressure further increased in this study. The decrease in D with increasing confining pressure, essentially determined by changes in the effective stress, was exponential. The methane diffusion coefficient of the cylindrical coal samples was similar to that of the permeability, and both decreased with increasing effective stress.

(2) The change in the methane diffusion coefficient with changing gas pressure in the cylindrical raw coal samples was opposite to that with changes in the confining pressure, increasing an exponential relationship. The rate of increase slowed with increasing gas pressure. D exponentially increased with a reduction in the effective stress caused by changes in the gas pressure; the rate of increase slightly slowed with a reduction in the effective stress. A limit exists on D under in situ geological conditions. The impact of gas pressure on D slightly differs from that of confining pressure, involving two mechanisms, mechanical action and adsorption, which are jointly constrained by the effective stress and changes in coal particle shrinkage/expansion. The two mechanisms lead to opposite results but are ultimately restricted by the main controlling factor: the mechanical effect of effective stress.

(3) The methane D of the raw coal cylindrical samples exponentially increased as the temperature increased, and the rate of increase only slightly increased with increasing temperature. The influence of temperature on diffusion is mainly achieved by changes in the root-mean-square speed and mean free path of the methane gas molecules.

(4) Under the same confining pressure, temperature, and gas pressure conditions for coal samples with the same degree of metamorphism, the methane D first increased and then decreased with an increase in the deformation degree, with the maximum D found in fractured coal. D and f of coal exhibited a nonlinear Holliday function variation, and D first increased and then decreased as the coal structure changed from simple to complex. Under similar deformation conditions, D of anthracite was larger than that of fat coal. Porosity is the key factor affecting changes in the methane diffusion coefficient of different metamorphic deformed coals.

Author Contributions: Conceptualization, Z.S.; Data curation, J.R., L.G., H.W., Y.Z., and B.L.; Formal analysis, J.R., L.G., H.W., and B.L.; Funding acquisition, J.R., Z.S., and B.L.; Investigation, Z.W., J.L., R.L., and Y.Q.; Methodology, J.R., L.G., and Z.S.; Supervision, Z.W., J.L., R.L., Y.Q., and Z.S.; Validation, J.R. and Z.W.; Writing—original draft, J.R.; Writing—review & editing, J.R. and B.L. All authors have read and agreed to the published version of the manuscript.

Funding: This research was funded by the National Natural Science Foundation of China (Grant Nos. 42002185, 41972177 and 42172189), the Natural Science Foundation of Henan province (No. 202300410099), the Key Scientific and Technological Project of Henan Province (No. 192102310464), the Key Research Project of Higher Education in Henan Province (No. 18A440008), and the Doctoral Scientific Fund Project of Henan University of Engineering (No. D2017010).

Institutional Review Board Statement: Not applicable.

Informed Consent Statement: Not applicable.

Data Availability Statement: The experimental data used to support the results of this study are available from the corresponding authors upon request.

Conflicts of Interest: The authors declare no conflict of interest.

References

1. Wang, X.L.; Pan, J.N.; Wang, K.; Mou, P.W.; Li, J.X. Fracture variation in high-rank coal induced by hydraulic fracturing using X-ray computer tomography and digital volume correlation. *Int. J. Coal Geol.* **2022**, *252*, 103942.
2. Wang, Q.W.; Guo, B.; Song, M.; Yan, Q. Construction and application of "coal-water-environment" coordinated development evaluation index system: A case study of Sihe Minefield. *Coal Geol. Explor.* **2022**, *50*, 98–105.
3. Ren, J.G.; Song, Z.M.; Li, B.; Liu, J.B.; Lv, R.S.; Liu, G.F. Structure feature and evolution mechanism of pores in different metamorphism and deformation coals. *Fuel* **2021**, *283*, 119292. [CrossRef]
4. Zhao, W.; Cheng, Y.P.; Pan, Z.J.; Wang, K.; Liu, S.M. Gas diffusion in coal particles: A review of mathematical models and their applications. *Fuel* **2019**, *252*, 77–100.
5. Zhang, Q.G.; Li, Q.S.; Fan, X.Y.; Liu, C.; Ge, Z.L.; Jiang, Z.G.; Peng, X.L.; Li, X.C.; Zhu, S.Y.; Zhao, S.L.; et al. Current situation and development trend of theories and technologies for coal and CBM co-mining in China. *Nat. Gas Ind.* **2022**, *42*, 130–145.
6. Wang, Z.Z.; Fu, X.H.; Hao, M.; Li, G.F.; Pan, J.N.; Niu, Q.H.; Zhou, H. Experimental insights into the adsorption-desorption of CH_4/N_2 and induced strain for medium-rank coals. *J. Pet. Sci. Eng.* **2021**, *204*, 108705.
7. Tao, S.; Pan, Z.J.; Tang, S.L.; Chen, S.D. Current status and geological conditions for the applicability of CBM drilling technologies in China: A review. *Int. J. Coal Geol.* **2019**, *202*, 95–108. [CrossRef]
8. Hu, B.; Cheng, Y.P.; Pan, Z.J. Classification methods of pore structures in coal: A review and new insight. *Gas Sci. Eng.* **2023**, *110*, 204876.
9. Zhou, H.; Wu, C.F.; Pan, J.N.; Wang, Z.Z.; Niu, Q.H.; Du, M.Y. Research on molecular structure characteristics of vitrinite and inertinite from bituminous coal with FTIR, Micro-Raman, and XRD spectroscopy. *Energy Fuel* **2021**, *35*, 1322–1335. [CrossRef]
10. Mou, P.W.; Pan, J.N.; Niu, Q.H.; Wang, Z.Z.; Li, Y.B.; Song, D.Y. Coal pores: Methods, types, and characteristics. *Energy Fuel* **2021**, *35*, 7467–7484. [CrossRef]
11. Liu, D.; Wang, Y.; Ni, X.; Tao, C.; Fan, J.; Wu, X.; Zhao, S. Classification of coal structure combinations and their influence on hydraulic fracturing: A case study from the Qinshui Basin, China. *Energies* **2020**, *13*, 4559. [CrossRef]
12. Li, Z.Q.; Li, P.F.; Wang, L.; Liu, Y.W.; Li, L. Experiment, model, and mechanism of multiscale dynamic diffusion–permeability in coal under different fluids. *ACS Omega* **2023**, *8*, 1606–1617. [CrossRef] [PubMed]
13. Ren, J.G.; Wang, Z.Z.; Li, B.; Chen, F.; Liu, J.B.; Liu, G.F.; Song, Z.M. Fractal-time-dependent Fick diffusion model of coal particles based on desorption–diffusion experiments. *Energy Fuel* **2022**, *36*, 6198–6215. [CrossRef]
14. Li, Z.Q.; Peng, J.S.; Li, L.; Qi, L.L.; Li, W. Novel dynamic multiscale model of apparent diffusion permeability of methane through low-permeability coal seams. *Energy Fuel* **2021**, *35*, 7844–7857. [CrossRef]
15. Pan, Z.J.; Connell, L.D.; Camilleri, M.; Connelly, L. Effects of matrix moisture on gas diffusion and flow in coal. *Fuel* **2010**, *89*, 3207–3217. [CrossRef]
16. Wen, Z.H.; Wang, Q.; Ren, J.G.; Zhang, L.L.; Yuan, Y.W. Dynamic gas diffusion model of capillary pores in a coal particle based on pore fractal characteristics. *Transp. Porous Media* **2021**, *140*, 581–601.
17. Wang, Y.; Liu, S.M. Estimation of pressure-dependent diffusive permeability of coal using methane diffusion coefficient: Laboratory measurements and modeling. *Energy Fuel* **2016**, *30*, 8968–8976. [CrossRef]
18. Xu, H.; Tang, D.Z.; Zhao, J.L.; Li, S.; Tao, S. A new laboratory method for accurate measurement of the methane diffusion coefficient and its influencing factors in the coal matrix. *Fuel* **2015**, *158*, 239–247.
19. Liu, J.J.; Cheng, D.Q.; Li, Y.L.; Zhao, K.; Kou, Q.Q. Quantitative evaluation of the influence of coal particle size distribution on gas diffusion coefficient by image processing method. *Fuel* **2022**, *314*, 122946. [CrossRef]
20. Liu, Z.D.; Lin, X.S.; Cheng, Y.P.; Chen, R.; Zhao, L.Y.; Wang, L.; Li, W.; Wang, Z.Y. Experimental investigation on the diffusion property of different form coal: Implication for the selection of CO_2 storage reservoir. *Fuel* **2022**, *318*, 123691.
21. Sander, R.; Connell, L.D.; Camilleri, M.C.; Pan, Z.J. CH_4, CO_2, N_2 diffusion in Bowen Basin (Australia) coal: Relationship between sorption kinetics of coal core and crushed coal particles. *J. Nat. Gas Sci. Eng.* **2020**, *81*, 103468. [CrossRef]
22. Bai, Y.; Lin, H.F.; Li, S.G.; Long, H.; Yan, M.; Li, Y.; Qin, L.; Zhou, B. Experimental study on kinetic characteristics of gas diffusion in coal under nitrogen injection. *Energy* **2022**, *254*, 124251. [CrossRef]
23. Tan, Y.L.; Pan, Z.J.; Liu, J.S.; Kang, J.H.; Zhou, F.B.; Connell, L.D.; Yang, Y.X. Experimental study of impact of anisotropy and heterogeneity on gas flow in coal. Part I: Diffusion and adsorption. *Fuel* **2018**, *232*, 444–453. [CrossRef]
24. Liu, Q.Q.; Wang, J.; Liu, J.J.; Yang, Q.Q.; Huang, W.Y.; Liu, Y.Y.; Wang, L. Determining diffusion coefficients of coal particles by solving the inverse problem based on the data of methane desorption measurements. *Fuel* **2022**, *308*, 122045. [CrossRef]
25. Lu, S.Q.; Li, M.J.; Sa, Z.Y.; Liu, J.; Wang, S.C.; Qu, M. Discrimination of gas diffusion state in intact coal and tectonic coal: Model and experiment. *Fuel* **2022**, *325*, 124916. [CrossRef]
26. An, F.H.; Jia, H.F.; Feng, Y. Effect of stress, concentration and temperature on gas diffusion coefficient of coal measured through a direct method and its model application. *Fuel* **2022**, *312*, 122991. [CrossRef]
27. Li, Y.D.; Pan, J.N.; Cheng, N.N.; Wang, Z.Z.; Zhang, L.; Liu, W.Q. Relationship between micropore structure of different coal ranks and methane diffusion. *Nat. Resour. Res.* **2022**, *31*, 2901–2917. [CrossRef]

28. Lu, X.; Armstrong, R.T.; Mostaghimi, P. Analysis of gas diffusivity in coal using micro-computed tomography. *Fuel* **2020**, *261*, 116384. [CrossRef]
29. Thimons, E.D.; Kissell, F.N. Diffusion of methane through coal. *Fuel* **1973**, *52*, 274–280. [CrossRef]
30. Sevenster, P.G. Diffusion of gases through coal. *Fuel* **1959**, *38*, 403–418.
31. Smith, D.M.; Williams, F.L. Diffusional effects in the recovery of methane from coalbeds. *Soc. Pet. Eng. J.* **1984**, *24*, 529–535. [CrossRef]
32. Meng, Y.; Li, Z.P. Experimental study on diffusion property of methane gas in coal and its influencing factors. *Fuel* **2016**, *185*, 219–228. [CrossRef]
33. Dong, J.; Cheng, Y.P.; Pan, Z.J. Comparison of transient and pseudo-steady diffusion of methane in coal and implications for coalbed methane control. *J. Pet. Sci. Eng.* **2020**, *184*, 106543. [CrossRef]
34. Baatar, L.; Mostaghimi, P.; Yuan, M.; Armstrong, R.T.; Adler, L.; Canbulat, I.; Si, G.Y.; Gaidarov, B.; Jing, Y. Multiscale measurements of gas diffusion coefficient of coal using counter-diffusion and image-based methods. *Int. J. Coal Geol.* **2023**, *265*, 104155. [CrossRef]
35. Liu, T.; Lin, B.Q.; Fu, X.H.; Gao, Y.B.; Kong, J.; Zhao, Y.; Song, H.R. Experimental study on gas diffusion dynamics in fractured coal: A better understanding of gas migration in in-situ coal seam. *Energy* **2020**, *195*, 117005. [CrossRef]
36. Qin, Y.J.; An, F.H.; Su, W.W.; Jia, H.F.; Chen, X.J. Direct determination of the diffusion coefficient variation of cylindrical coal based on Fick's law and model construction. *Coal Sci. Technol.* **2023**, *51*, 1–10.
37. Yi, M.H.; Wang, L.; Cheng, Y.P.; Wang, C.H.; Hu, B. Calculation of gas concentration-dependent diffusion coefficient in coal particles: Influencing mechanism of gas pressure and desorption time on diffusion behavior. *Fuel* **2022**, *320*, 123973. [CrossRef]
38. Fang, X.L.; Liu, D.L.; Zhou, Y.F.; Liu, X.B.; Cai, Y.D. Factors influencing methane diffusion behaviors in micro-nano coal pores: A comprehensive study. *Front. Earth Sci.* **2023**, *17*, 71–86. [CrossRef]
39. Song, H.R.; Lin, B.Q.; Zhong, Z.; Liu, T. Experimental study on methane diffusion kinetics in three typical metamorphic coals. *Fuel* **2022**, *311*, 122601. [CrossRef]
40. Cheng, Y.P.; Pan, Z.J. Reservoir properties of Chinese tectonic coal: A review. *Fuel* **2020**, *260*, 116350.
41. Yang, X.; Wang, G.D.; Zhang, J.Y.; Ren, T. The influence of sorption pressure on gas diffusion in coal particles: An experimental study. *Processes* **2019**, *7*, 219. [CrossRef]
42. Zang, J.; Wang, K.; Liu, A. Phenomenological over-parameterization of the triple-fitting-parameter diffusion models in evaluation of gas diffusion in coal. *Processes* **2019**, *7*, 241. [CrossRef]
43. Liu, Q.Q.; Huang, W.Y.; Lv, B.; Ma, X.H.; Lu, X.D.; Wang, J.; Wang, L. Decoupling experiments for CH_4 "diffusion-seepage" in coal columns to effectively measure sorption time. *Int. J. Coal Geol.* **2022**, *261*, 104074. [CrossRef]
44. Cai, Y.Y.; Cheng, J.S.; Cheng, B. Study on the gas emission law of circular column cinder based on time–varying diffusion coefficient. *Min. Saf. Environ. Prot.* **2020**, *47*, 32–36.
45. Song, Y.; Jiang, B.; Li, M.; Hou, C.L.; Xu, S.C. A review on pore-fractures in tectonically deformed coals. *Fuel* **2020**, *278*, 118248.
46. *GB/T 6948-2008*; Chinese National Standard. Method of Determining Microscopically the REFLECTANCE of vitrinite on Coal. Standardization Administration of China: Beijing, China, 2008. (In Chinese)
47. *GB/T 212-2008*; Chinese National Standard. Proximate Analysis of Coal. Standardization Administration of China: Beijing, China, 2008. (In Chinese)
48. *GB/T 23561.4-2009*; Chinese National Standard. Methods for Determining the Physical and Mechanical Properties of Coal and Rock. Part 4: Methods for Calculating the Porosity of Coal and Rock. Standardization Administration of China: Beijing, China, 2009. (In Chinese)
49. *GB/T 23561.12-2010*; Chinese National Standard. Methods for Determining the Physical and Mechanical Properties of Coal and Rock. Part 12: Methods for Determining Coal Hardiness Coefficient. Standardization Administration of China: Beijing, China, 2010. (In Chinese)
50. Ren, J.G.; Weng, H.B.; Song, Z.M.; Li, B.; Lv, R.S. Method of making raw coal isostatic pressing columnar coal samples for heavily tectonically deformed coal. *Saf. Coal Mines* **2018**, *49*, 66–69.
51. Liu, G.F. Mechanism and Model of Coal Adsorption Gas in High Temperature and Pressure and Three-Phase Medium. Ph.D. Thesis, Henan Polytechnic University, Jiaozuo, China, 2011.
52. Zhu, W.C.; Liu, S.Y.; Zhang, X.F.; Wei, C.H. Coupled coal–gas interaction during CBM and CO_2-ECBM recovery in coal seams: A critical review. *Geomech. Geophys. Geo-Energy Geo-Resour.* **2022**, *8*, 195.
53. Liu, Z.D.; Lin, X.S.; Wang, Z.Y.; Zhang, Z.; Chen, R.; Wang, L.; Li, W. Modeling and experimental study on methane diffusivity in coal mass under in-situ high stress conditions: A better understanding of gas extraction. *Fuel* **2022**, *321*, 124078. [CrossRef]
54. Niu, Q.H.; Cao, L.W.; Sang, S.X.; Zhou, X.Z.; Wang, W.; Yuan, W.; Ji, Z.M.; Wang, H.C.; Nie, Y. Study on the anisotropic permeability in different rank coals under influences of supercritical CO_2 adsorption and effective stress and its enlightenment for CO_2 enhance coalbed methane recovery. *Fuel* **2020**, *262*, 116515. [CrossRef]
55. Ji, X.F.; Song, D.Y.; Shi, W.F.; Li, Y.F. Influence of nanopore structure deformation on gas migration in coal. *ACS Omega* **2021**, *29*, 19115–19126. [CrossRef]
56. Wang, Z.Z.; Fu, X.H.; Pan, J.N.; Deng, Z. Effect of N_2/CO_2 injection and alternate injection on volume swelling/shrinkage strain of coal. *Energy* **2023**, *275*, 127377. [CrossRef]
57. Zhao, D.; Li, X.W.; Feng, Z.C.; Pu, Y.X.; Chang, H.M.; Jia, Y.C. Study on the behavior and mechanism of methane desorption-diffusion for multi-scale coal samples under multi-temperature conditions. *Fuel* **2022**, *328*, 125332. [CrossRef]

58. Qin, Y.P.; Xu, H.; Yang, D.Y.; Sun, Y.; Guo, M.Y.; Zhang, F.J.; Wu, F.; Li, Y.W.; Fan, J.F. Modeling of gas desorption and diffusion kinetics in a coal seam combined with a free gas density gradient concept. *Energy Fuel* **2022**, *36*, 10052–10063.
59. Liu, S.; Wei, C.; Zhu, W.; Zhang, M. Temperature- and pressure-dependent gas diffusion in coal particles: Numerical model and experiments. *Fuel* **2020**, *266*, 117054. [CrossRef]
60. Liu, Y.W.; Du, Y.; Li, Z.Q.; Zhao, F.J.; Zuo, W.Q.; Wei, J.P.; Mitri, H. A rapid and accurate direct measurement method of underground coal seam gas content based on dynamic diffusion theory. *Int. J. Min. Sci. Technol.* **2020**, *30*, 799–810.
61. Lu, S.Q.; Wang, C.F.; Li, M.J.; Sa, Z.Y.; Zhang, Y.L.; Liu, J.; Wang, H.; Wang, S.C. Gas time-dependent diffusion in pores of deformed coal particles: Model development and analysis. *Fuel* **2021**, *295*, 120566. [CrossRef]
62. Qin, Y.; Xu, H.; Liu, W.; Liu, J.; Duan, W. Time- and pressure-independent gas transport behavior in a coal matrix: Model development and improvement. *Energy Fuel* **2020**, *34*, 9355–9370. [CrossRef]